AN ADAPTIVE NEWTON-METHOD
BASED ON A DYNAMICAL SYSTEMS APPROACH

MARIO AMREIN AND THOMAS P. WIHLER

ABSTRACT. The traditional Newton method for solving nonlinear operator equations in Banach spaces is discussed within the context of the continuous Newton method. This setting makes it possible to interpret the Newton method as a discrete dynamical system and thereby to cast it in the framework of an adaptive step size control procedure. In so doing, our goal is to reduce the chaotic behavior of the original method without losing its quadratic convergence property close to the roots. The performance of the modified scheme is illustrated with various examples from algebraic and differential equations.

1. INTRODUCTION

Let X, Y be two Banach spaces, with norms $\|\cdot\|_X$ and $\|\cdot\|_Y$, respectively. Given an open subset $\Omega \subset X$, and a continuous (possibly nonlinear) operator $\mathsf{F} : \Omega \to Y$, we are interested in finding the zeros $x \in \Omega$ of F, i.e., we aim to solve the operator equation

$$x \in \Omega : \qquad \mathsf{F}(x) = 0. \tag{1}$$

Supposing that the Fréchet derivative F' of F exists in Ω (or in a suitable subset), the classical Newton-Raphson method for solving (1) starts from an initial guess $x_0 \in \Omega$, and generates the iterates

$$x_{n+1} = x_n + \delta_n, \tag{2}$$

where the update $\delta_n \in X$ is implicitly given by the *linear* equation

$$\mathsf{F}'(x_n)\delta_n = -\mathsf{F}(x_n),$$

for $n \geq 0$. Naturally, we need to assume that $\mathsf{F}'(x_n)$ is invertible for all $n \geq 0$, and that $\{x_n\}_{n \geq 0} \subset \Omega$.

Newton's method features both local as well as global properties. On the one hand, on a *local* level, the scheme is often celebrated for its quadratic convergence regime 'sufficiently close' to a root. From a *global* perspective, on the other hand, the Newton method is well-known to exhibit chaotic behavior. Indeed, the original works of Fatou [4] and Julia [5], for instance, revealed that applying the Newton method to algebraic systems of equations may result in highly complex or even fractal attractor boundaries of the associated roots. This was confirmed in the 1980s when computer graphics were employed to illustrate the theoretical results numerically; see, e.g., [13].

In order to tame the chaotic behavior of Newton's method a number of different ideas have been proposed in the literature. In particular, the use of damping aiming to avoid the appearance of possibly large updates in the iterations, constitutes a popular approach in practical applications. More precisely, (2) is replaced with

$$x_{n+1} = x_n + \alpha \delta_n,$$

for a possibly small damping parameter $0 < \alpha < 1$. More sophisticatedly, variable damping may lead to more efficient results; see, e.g., the extensive overview [1] or [2, 3, 16] for different variations of the classical Newton scheme. The idea of adaptively adjusting the magnitude of the Newton updates has also been studied in the recent article [14]; there, following, e.g., [9, 13, 15], the Newton method was identified as the numerical discretization of a specific ordinary differential equation (ODE)—the so-called continuous Newton method—by the explicit Euler scheme, with a fixed step size $h = 1$. Then, in order to tame the chaotic behavior of the Newton iterations, the idea presented in [14] is based on discretizing the continuous Newton ODE by the explicit Euler method with variable step sizes, and to combine it with a simple step size control procedure; in particular, the resulting procedure retains the optimal step size 1 whenever sensible and is able to deal with singularities in the iterations more carefully than the classical Newton scheme. In fact, numerical experiments revealed that the new method is able to generate attractors with almost smooth boundaries where the traditional Newton method produces fractal Julia sets. Moreover, the numerical tests demonstrated an improved convergence rate not matched on average by the classical Newton method.

The goal of the present paper is to continue the work in [14] on simple algebraic systems, and to extend it to the context of general Banach spaces; in particular, nonlinear boundary value problems will be focused on, and an empirical investigation demonstrating the ability of the proposed approach to tame chaos in attractor boundaries will be provided in such situations. Furthermore, in contrast to the adaptive control mechanism in [14], which is based on an intermediate step technique, we develop and test a pure prediction scheme in the present article. This will make it possible to compute the individual iterations much more efficiently. Indeed, this is most relevant in more complex applications such as in the numerical approximation of nonlinear ordinary and partial differential equations.

Finally, let us remark that there is a large application and research area where methods related to the continuous version of the Newton method are considered in the context of nonlinear optimization. Some of these schemes count among the most efficient ones available for special purposes; see, e.g., [12] and the references therein for details.

2. An Adaptive Newton Method

The aim of this section is to develop an adaptive Newton method based on a simple prediction strategy. To this end, we will first recall the continuous Newton ODE.

2.1. Discrete vs. Continuous Newton Method.
In order to improve the convergence behavior of the (*discrete*) Newton method (2) in the case that the initial guess is far away from a root $x_\infty \in \Omega$, it is classical to consider a damped version of the Newton sequence. More precisely, given a possibly small $t_n > 0$, we consider

the iteration

$$x_{n+1} = x_n - t_n \mathsf{F}'(x_n)^{-1}\mathsf{F}(x_n). \tag{3}$$

Rearranging terms results in

$$\frac{x_{n+1} - x_n}{t_n} = -(\mathsf{F}'(x_n))^{-1}\mathsf{F}(x_n),$$

we observe that (3) can be seen as the discretization of the initial value problem

$$\begin{cases} \dot{x}(t) = \mathsf{N}_\mathsf{F}(x(t)), & t \geq 0, \\ x(0) = x_0, \end{cases} \tag{4}$$

by the explicit Euler scheme with step size t_n. Here, $\mathsf{N}_\mathsf{F}(x) = -\mathsf{F}'(x)^{-1}\mathsf{F}(x)$ is the so-called Newton Raphson transform (NRT, for short; see [14]) of F. The system (4) is called *continuous Newton method*. It is noteworthy that, if N_F is of class C^1 on some neighborhood of $x_\infty \in \Omega$, then we have $\mathsf{D}(\mathsf{N}_\mathsf{F})(x_\infty) = -\mathsf{Id}$. In particular, by the Poincaré-Ljapunow Theorem (see, e.g., [17]) we conclude that each regular zero of F is located in an attracting neighborhood contained in Ω when the NRT is applied. Furthermore, hoping that a sufficiently smooth solution of (4) exists, and that $\lim_{t\to\infty} x(t) = x_\infty \in \Omega$ is well-defined with $\mathsf{F}(x_\infty) = 0$, one can readily infer that

$$\mathsf{F}(x(t)) = \mathsf{F}(x_0)e^{-t}. \tag{5}$$

The solvability of (4) within the framework of Banach spaces has been addressed in [10, 11]. Note that the trajectory of a solution of (4) either ends at the solution point x_∞ which is located closest to the initial value x_0, or at a some point close to a critical point x_c with non-invertible derivative F', or at some point on the boundary $\partial\Omega$ of the domain of F; see [7, 8].

Given an approximation $x_0 \in \Omega$ of a solution $x_\infty \in \Omega$ of (1), the basic idea in the design of the chaos-taming adaptive Newton scheme in this article is to provide some discrete dynamics which stay sufficiently close to the trajectories of the continuous Newton method leading to the root x_∞. Here, it is useful to take a global view: Instead of considering only one specific trajectory that transports an initial guess x_0 to x_∞, we consider the global flow Φ generated by the *Newton-field* N_F. That is, for $x \in \Omega$, we concentrate on the system

$$\begin{cases} \dot{\Phi}(t, x) = \mathsf{N}_\mathsf{F}(\Phi(t, x)), & t \geq 0, \\ \Phi(0, x) = x. \end{cases} \tag{6}$$

For a given root x_∞ of F we may now consider the set

$$\mathcal{A}(x_\infty) = \left\{ x_0 \in \Omega : \lim_{t\to\infty} \|\Phi(t, x_0) - x_\infty\|_X = 0 \right\} \tag{7}$$

of all points which belong to trajectories of (6) leading to x_∞. We note that the discrete dynamics as described by the Newton iteration (3) are based on possibly small but non-infinitesimal step sizes $t_n > 0$. In particular, the discrete iterates approximate the continuous trajectories from (6) and may therefore jump back and forth between them. The chaotic behavior of the discrete Newton method is tamed as long as the iterates stay within the *same* attractor $\mathcal{A}(x_\infty)$. Here, it is important to note that this is achievable in principle as long as the step sizes $t_n > 0$ are sufficiently small. Indeed, provided that Φ is continuous and that x_∞ is a regular zero of F which is contained in an attractive neighbourhood $B_\eta(x_\infty) \subset \mathcal{A}(x_\infty)$, for some $\eta > 0$, this simply follows from the fact that $\mathcal{A}(x_\infty)$ is an open set: To

see this, we choose any $x_0 \in \mathcal{A}(x_\infty)$; then, there exists $t > 0$ such that $\Phi(t, x_0) \in B_\eta(x_\infty)$. The openess of $B_\eta(x_\infty)$ together with the continuity of Φ implies the existence of some $\varepsilon, \delta > 0$ such that $\Phi(t, B_\delta(x_0)) \subset B_\varepsilon(\Phi(t, x_0)) \subset B_\eta(x_\infty)$, i.e., $B_\delta(x_0) \subset \mathcal{A}(x_\infty)$.

2.2. A Prediction Strategy.

In this section we discuss the linearization of the Newton-field $\mathsf{N_F}$ which will serve as a prediction strategy of the exact trajectories given in (6). We propose an adaptive path-following algorithm in such a way that, for a given initial guess $x_0 \in \mathcal{A}(x_\infty)$, the iterates $\{x_n\}_{n \in \mathbb{N}}$ presumably stay within $\mathcal{A}(x_\infty)$.

To simplify matters we fix $x(t) = \Phi(t, x_0)$ for $x_0 \in \mathcal{A}(x_\infty)$ and denote by $\hat{x}$ the linearization at $t = 0$, $x(0) = x_0$, i.e.

$$\hat{x}(t) = x_0 + t\dot{x}(0). \tag{8}$$

By the openess of $\mathcal{A}(x_\infty)$ we note that, for sufficiently small $t > 0$, there holds $\hat{x}(t) \in \mathcal{A}(x_\infty)$. Let us focus on the distance between $x(t)$ and its linearization $\hat{x}(t)$: In view of (4) and (8) we have that

$$
\begin{aligned}
\hat{x}(t) - x(t) &= \int_0^t \left(\dot{\hat{x}}(s) - \dot{x}(s) \right) \mathsf{d}s \\
&= \int_0^t \left(\mathsf{N_F}(x_0) - \mathsf{N_F}(x(s)) \right) \mathsf{d}s \\
&= \int_0^t \left(\mathsf{N_F}(x_0) - \mathsf{N_F}(x_0)e^{-s} \right) \mathsf{d}s + \int_0^t \left(\mathsf{N_F}(x_0)e^{-s} - \mathsf{N_F}(x(s)) \right) \mathsf{d}s \\
&= \mathsf{N_F}(x_0)(t + e^{-t} - 1) + I(t),
\end{aligned}
\tag{9}
$$

with

$$I(t) = \int_0^t \left(\mathsf{N_F}(x_0)e^{-s} - \mathsf{N_F}(x(s)) \right) \mathsf{d}s.$$

Using (5) we obtain

$$\mathsf{F}'(x_0)^{-1} \frac{\mathsf{d}}{\mathsf{d}s} \mathsf{F}(x(s)) = \mathsf{F}'(x_0)^{-1} \frac{\mathsf{d}}{\mathsf{d}s} \left(\mathsf{F}(x_0)e^{-s} \right) = -\mathsf{F}'(x_0)^{-1}\mathsf{F}(x_0)e^{-s} = \mathsf{N_F}(x_0)e^{-s}.$$

Thus, recalling (4), we get

$$
\begin{aligned}
I(t) &= \int_0^t \left(\mathsf{F}'(x_0)^{-1} \frac{\mathsf{d}}{\mathsf{d}s} \mathsf{F}(x(s)) - \dot{x}(s) \right) \mathsf{d}s \\
&= \mathsf{F}'(x_0)^{-1}(\mathsf{F}(x(t)) - \mathsf{F}(x_0)) - x(t) + x_0.
\end{aligned}
$$

A Taylor expansion for F about x_0 is given by

$$
\begin{aligned}
\mathsf{F}'(x_0)^{-1} &(\mathsf{F}(x(t)) - \mathsf{F}(x_0)) \\
&= \mathsf{F}'(x_0)^{-1} \left(\mathsf{F}(x_0) + \mathsf{F}'(x_0)(x(t) - x_0) + \mathcal{O}(\|x(t) - x_0\|_X^2) - \mathsf{F}(x_0) \right) \\
&= x(t) - x_0 + \mathcal{O}(\|x(t) - x_0\|_X^2).
\end{aligned}
$$

In particular, we see that $I(t) = \mathcal{O}(\|x(t) - x_0\|_X^2)$. Going back to (9) we arrive at

$$\hat{x}(t) - x(t) = \mathsf{N_F}(x_0)(t + e^{-t} - 1) + \mathcal{O}(\|x(t) - x_0\|_X^2).$$

We see that by neglecting the term $\mathcal{O}(\|x(t) - x_0\|_X^2)$, the expression $\mathsf{N}_\mathsf{F}(x_0)(t + e^{-t} - 1)$ is a computable quantity and can be used as an error indicator in each iteration step. Moreover, using that $e^{-t} = 1 - t + \frac{1}{2}t^2 + \mathcal{O}(t^3)$, it follows that

$$\hat{x}(t) - x(t) = \frac{1}{2}t^2 \mathsf{N}_\mathsf{F}(x_0) + \mathcal{O}(t^3) + \mathcal{O}(\|x(t) - x_0\|_X^2).$$

Thence, fixing a tolerance $\tau > 0$ such that

$$\tau = \|\hat{x}(t) - x(t)\|_X = \frac{t^2}{2}\|\mathsf{N}_\mathsf{F}(x_0)\|_X + \mathcal{O}(t^3) + \mathcal{O}(\|x(t) - x_0\|_X^2),$$

and ignoring the higher order approximation terms, motivates the following adaptive step size control procedure for the Newton iteration:

Algorithm 2.1. Fix a tolerance $\tau > 0$.
  i) Start the Newton iteration with an initial guess $x_0 \in \mathcal{A}(x_\infty)$.
  ii) In each iteration step $n = 0, 1, 2, \ldots$, compute

$$t_n = \min\left(\sqrt{\frac{2\tau}{\|\mathsf{N}_\mathsf{F}(x_n)\|_X}}, 1\right). \tag{10}$$

  iii) Compute x_{n+1} based on the Newton iteration (3), and go to the next step $n \leftarrow n + 1$.

Remark 2.2. The minimum in (10) is chosen such that $t_n = 1$ whenever possible, in particular, close to a root. This will retain the celebrated quadratic convergence property of the Newton scheme (provided that the corresponding root is simple).

Remark 2.3. Since we fix τ a priori it might happen that the step size t_n from (10) may be too large in the sense that the Newton sequence $\{x_n\}_{n\in\mathbb{N}}$ leaves the attractor $\mathcal{A}(x_\infty)$. Indeed, our Algorithm 2.1 obviously lacks a correction strategy for the predicted step size. This is in contrast to the references [1, 14] in the context of finite-dimensional algebraic systems, where the reduction of the step size may possibly be corrected in order for the iterates to stay within $\mathcal{A}(x_\infty)$. Evidently, however, a possible repeated reduction of the step size may strongly increase the computational complexity. Indeed, in view of solving nonlinear operator equations in infinite dimensional Banach spaces (by means of suitable discretization schemes), which are of interest in this work, a corresponding procedure might become unfeasibly expensive in practical applications.

2.3. **A Convergence Result.** We close this section by casting the rather geometrically inspired prediction path-following Algorithm 2.1 into a framework of a global analysis. There are various approaches that have been presented in the literature. Here, we follow along the lines of [1], and show that the residuum $\mathsf{F}(x_n) \to 0$ as $n \to \infty$ if certain (quite strong) conditions hold. Specifically, we assume that, for given $\tau > 0$ and $x_0 \in \Omega$, the Newton sequence $\{x_n\}_{n\geq 0}$ defined in (3) with t_n from (10) satisfies the following properties:
(A) The sequence $\{x_n\}_{n\geq 0}$ is well-defined, i.e., in particular, for any $n \geq 0$, we have that $x_n \in \Omega$, and $\mathsf{F}'(x_n)$ is invertible.
(B) There exists a constant $\hat{K} > 0$ such that $\left\|\mathsf{F}'(x_n)^{-1}\right\|_{Y\to X} \leq \hat{K}$ for all $n \geq 0$.
(C) There is a compact set $M \subset \Omega$ as well as a constant $\tilde{K} > 0$ such that the piecewise linear trajectory connecting the points $x_0, x_1, x_2, \ldots$ is contained in M and such that $\|\mathsf{F}'(x) - \mathsf{F}'(y)\|_{X\to Y} \leq \tilde{K}\|x - y\|_X$ for all $x, y \in M$.

Theorem 2.4. *Let $x_0 \in \Omega$, and suppose that there exists $\tau_0 > 0$ such that the properties (A)–(C) above are fulfilled for any $\tau \leq \tau_0$. Then, for*

$$0 < \tau < \min\left\{\tau_0, \frac{2}{\hat{K}^2\tilde{K}^2}\inf_{n\geq 0}\|\mathsf{N}_\mathsf{F}(x_n)\|_X^{-1}, \hat{K}^{-1}\tilde{K}^{-1}\right\}, \tag{11}$$

the adaptive Newton iteration (3), with t_n from (10), $n \geq 0$, converges, i.e., it holds that $\lim_{n\to\infty}\|\mathsf{F}(x_n)\|_X = 0$.

Remark 2.5. We note that, for all $n \geq 0$, we have that

$$\|\mathsf{N}_\mathsf{F}(x_n)\|_X \leq \left\|\mathsf{F}'(x_n)^{-1}\right\|_{Y\to X}\|\mathsf{F}(x_n)\|_Y \leq \hat{K}\sup_{x\in M}\|\mathsf{F}(x)\|_Y < \infty. \tag{12}$$

The last inequality follows from the fact that M is compact and that the mapping $x \mapsto \|\mathsf{F}(x)\|_Y$ is continuous on M. As a consequence, the set $\{\|\mathsf{F}(x)\|_Y : x \in M\}$ is compact in $\mathbb{R}$, and hence bounded and closed. In particular, the supremum in (12) is attained and bounded. Thus, if $\mathsf{F} \not\equiv 0$ on M,

$$\inf_{n\geq 0}\|\mathsf{N}_\mathsf{F}(x_n)\|_X^{-1} \geq \hat{K}^{-1}\left(\sup_{x\in M}\|\mathsf{F}(x)\|_Y\right)^{-1} > 0.$$

Especially, it is possible to choose $\tau > 0$ in (11).

Remark 2.6. We note that the assumptions in Theorem 2.4 are of a theoretical nature and difficult to check in general. From a heuristic point of view, however, our result illustrates that convergence of the Newton sequence to a zero of F is reasonable to achieve, provided that τ is chosen sufficiently small.

Proof of Theorem 2.4. Let $\tau > 0$ satisfy (11). Then, we choose $\epsilon > 0$ such that

$$0 < \tau(1+\epsilon)^2 \leq \min\left\{\tau_0, \frac{2}{\hat{K}^2\tilde{K}^2}\inf_{n\geq 0}\|\mathsf{N}_\mathsf{F}(x_n)\|_X^{-1}, \hat{K}^{-1}\tilde{K}^{-1}\right\}.$$

By the mean value theorem we have

$$\mathsf{F}(x_1) - \mathsf{F}(x_0) = \mathsf{F}(x_0 + t_0\mathsf{N}_\mathsf{F}(x_0)) - \mathsf{F}(x_0) = \left(\int_0^{t_0}\mathsf{F}'(x_0 + s\mathsf{N}_\mathsf{F}(x_0))\,\mathsf{d}s\right)\mathsf{N}_\mathsf{F}(x_0).$$

Hence,

$$\mathsf{F}(x_1) = \mathsf{F}(x_0)(1 - t_0) + \left(\int_0^{t_0}(\mathsf{F}'(x_0 + s\mathsf{N}_\mathsf{F}(x_0)) - \mathsf{F}'(x_0))\,\mathsf{d}s\right)\mathsf{N}_\mathsf{F}(x_0).$$

In particular, recalling condition (C) above, we notice that the previous integrals are all well-defined. By definition, we have that $t_0 \in (0,1]$, and thus, employing the triangle inequality, we obtain the estimate

$$\|\mathsf{F}(x_1)\|_Y \leq (1 - t_0)\|\mathsf{F}(x_0)\|_Y$$
$$+ \left\|\int_0^{t_0}(\mathsf{F}'(x_0 + s\mathsf{N}_\mathsf{F}(x_0)) - \mathsf{F}'(x_0))\,\mathsf{d}s\right\|_{X\to Y}\|\mathsf{N}_\mathsf{F}(x_0)\|_X \tag{13}$$
$$\leq (1 - t_0)\|\mathsf{F}(x_0)\|_Y + \frac{t_0^2}{2}\tilde{K}\|\mathsf{N}_\mathsf{F}(x_0)\|_X^2 \leq \gamma_0\|\mathsf{F}(x_0)\|_Y,$$

where

$$\gamma_0 = 1 - t_0 + \frac{t_0^2}{2}K\|\mathsf{N}_\mathsf{F}(x_0)\|_X,$$

for $K = \hat{K}\tilde{K}$. In order to estimate γ_0, we consider two cases:

Case 1: Let first
$$\frac{2\tau}{\|N_F(x_0)\|_X} \geq 1.$$

Then, $t_0 = 1$ in (10), and $\|N_F(x_0)\|_X \leq 2\tau$. Therefore,
$$\gamma_0 = \frac{1}{2}K\,\|N_F(x_0)\|_X \leq K\tau.$$

Using that
$$\tau(1+\epsilon) < \tau(1+\epsilon)^2 \leq K^{-1}, \tag{14}$$

results in
$$\gamma_0 < \frac{1}{1+\epsilon} < 1.$$

Case 2: If secondly,
$$\frac{2\tau}{\|N_F(x_0)\|_X} < 1,$$

then
$$t_0 = \sqrt{\frac{2\tau}{\|N_F(x_0)\|_X}} \geq \sqrt{2\tau\,\inf_{n\geq 0}\|N_F(x_n)\|_X^{-1}}.$$

Noticing that
$$\tau \leq \frac{2}{K^2(1+\epsilon)^2}\,\inf_{n\geq 0}\|N_F(x_n)\|_X^{-1},$$

or equivalently,
$$\inf_{n\geq 0}\|N_F(x_n)\|_X^{-1} \geq \frac{\tau K^2(1+\epsilon)^2}{2},$$

we arrive that
$$t_0 \geq \tau K(1+\epsilon).$$

In this way, we obtain
$$\gamma_0 = 1 - t_0 + K\tau \leq 1 - \tau K(1+\epsilon) + K\tau \leq 1 - K\tau\epsilon.$$

Recalling (14), we see that $0 < K\tau\epsilon < \epsilon(1+\epsilon)^{-1} < 1$.

In summary, we see that $\gamma_0 \leq q$, where $q = \max\left(1 - K\tau\epsilon, (1+\epsilon)^{-1}\right) \in (0,1)$. It follows from (13) that $\|F(x_1)\|_X \leq q\,\|F(x_0)\|_X$. By induction, we conclude that
$$\|F(x_n)\|_X \leq q^n\,\|F(x_0)\|_X \to 0,$$

with $n \to \infty$. This completes the proof. $\qquad\square$

3. APPLICATIONS

The purpose of this section is to illustrate Algorithm 2.1 by means of a number of examples. In particular, we will focus on nonlinear algebraic systems and on differential equations.
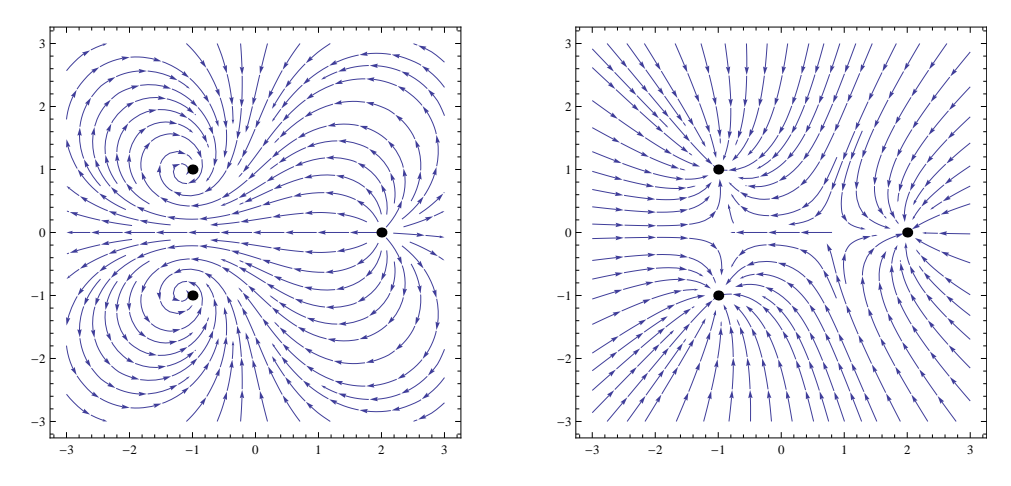
FIGURE 1. The direction fields corresponding to $\mathsf{F}(z) = z^3 - 2z - 4$ (left) and to the NRT (right).

3.1. **Algebraic equations.** Let us look at two algebraic problems. The first one is a cubic polynomial equation on $\mathbb{C}$ (identified with $\mathbb{R}^2$) with three separate zeros, and the second example is a challenging benchmark problem in $\mathbb{R}^2$.

Example 3.1. We consider the function

$$\mathsf{F} : \mathbb{C} \to \mathbb{C}, \qquad z \mapsto \mathsf{F}(z) = z^3 - 2z - 4, \tag{15}$$

with the three zeros

$$Z_{\mathsf{F}} = \{(2, 0), (-1, 1), (-1, -1)\} \subset \mathbb{C}.$$

We observe that F' vanishes at $\left(\pm\sqrt{2/3}, 0\right)$. This causes large updates in the Newton iteration close to those points, and hence, a source of potential chaos has been generated by applying the NRT; cf. [14, Example 2]. In order to discuss the behavior of the Newton method for this example, let us first focus on the vector fields corresponding to F and N_{F}; see Figure 1 left and right, respectively. One can clearly see that the root $(2, 0) \in Z_{\mathsf{F}}$ is repulsive for F. Moreover, the zeros $\{(-1, 1), (-1, -1)\} \in Z_{\mathsf{F}}$ of F show a curl. For N_{F} the situation is completely different: All the three roots are attractive, and the vectors point directly to the three roots of F. Therefore, the NRT N_{F} can be used to transport an initial guess $x_0 \in \mathcal{A}(x_\infty)$ arbitrarily close to a root x_∞. In the given example, we observe that the vector direction field is divided into three different sectors for N_{F}, which are the attractors for the initial value problem (4).

In Figure 2 we display the behavior of the classical (with step size $t_n = 1$), the continuous, and the adaptive Newton method (with $\tau = 0.05$ and t_n from (10)), for the initial point $x_0 = (0.08, 0.55)$. We see that, while the classical solution shows large updates and thereby leaves the original attractor, the iterates corresponding to the adaptive Newton method follow the exact solution (which is approximated by a numerical reference solution with $t \ll 1$) quite closely and approach the "correct" zero.

In order to visualize the domains of attraction of different Newton schemes, we compute the zeros of F by sampling initial values on a 1001×1001 grid in the domain
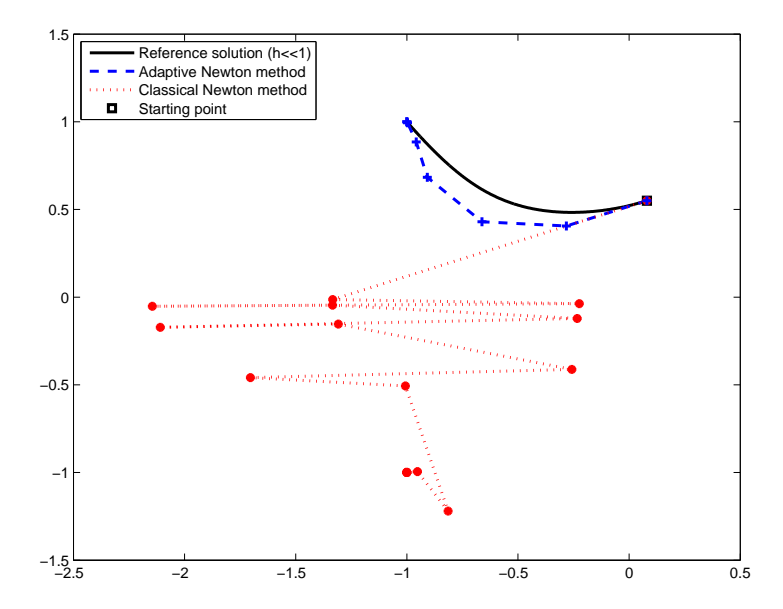
FIGURE 2. Performance of the classical Newton and the Newton method with adaptive step size control (with $\tau = 0.05$) for the starting point $x_0 = (0.08, 0.55)$.

$[-5, 5] \times [-5, 5]$. In Figure 3, we show the fractal generated by the traditional Newton method with constant step size 1 (left) as well as the corresponding plot for the damped Newton scheme with constant step size 0.72. We observe that the damped Newton method is able to control the chaos to some extent, however, there are still relatively large fractal areas. Furthermore, in Figure 4, we use adaptive step size control based on Algorithm 2.1 by setting $\tau = 0.1$ (left) and $\tau = 0.001$ (right). The chaotic behavior caused by the singularities of F' is clearly tamed by the adaptive Newton method.

Comparing the statistics resulting from a step size control computation with $\tau = 0.1$ with the corresponding results for a fixed step size underlines the superiority of the proposed approach; see the performance data in Table 1. The information is based on 10^4 starting values in the domain $[-5, 5] \times [-5, 5]$. We list the percentage of convergent iterations, the average number of iterations necessary to obtain an absolute accuracy of at least 10^{-8}, and the average convergence rate defined as follows: The error in the n-th iteration, that is

$$e_n = \|x_\infty - x_n\|, \qquad x_\infty \in Z_\mathsf{F},$$

is supposed to satisfy a relation of the form

$$e_n = ce_{n-1}^\rho \qquad \Leftrightarrow \qquad \ln(e_n) = C + \rho \ln(e_{n-1}), \quad n \in \mathbb{N}, \tag{16}$$

for a constant ρ. This is the rate of convergence, which, for $n \to \infty$, will typically tend to a stable limit. Clearly, due to finite resources, we can determine ρ only empirically, i.e., we denote by $\tilde\rho$ the convergence rate that we will obtain by applying a least squares approximation to (16) (averaged over all computed iterations) for the unknown parameters ρ resp. C. A starting value x_0 is called convergent if it is in fact convergent and, additionally, approaches the "correct zero", i.e. the zero that
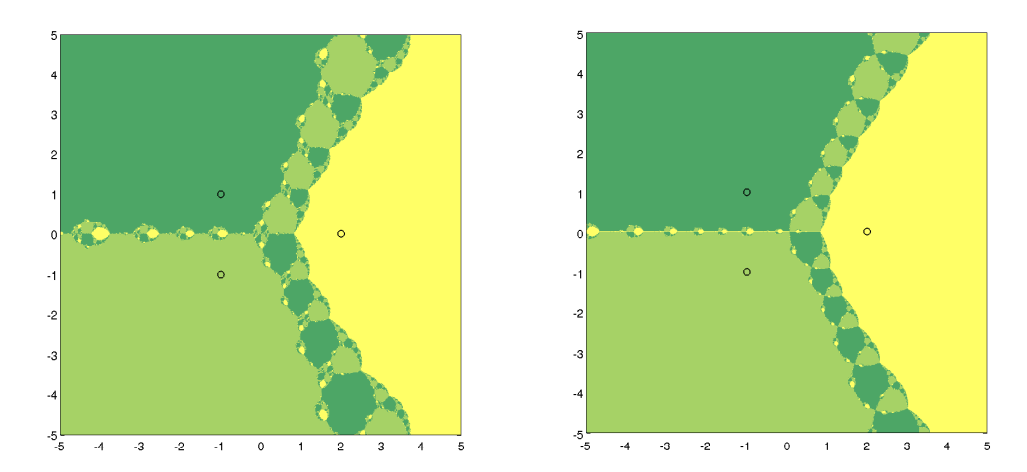
FIGURE 3. The basins of attraction for $z^3 - 2z - 4 = 0$ by the Newton method: The classical scheme on the left (i.e., $t = 1$), and on the right with a fixed reduced step size ($t = 0.72$). Three different colors distinguish the three basins of attraction associated with the three solutions (each of them is marked by a small circle).
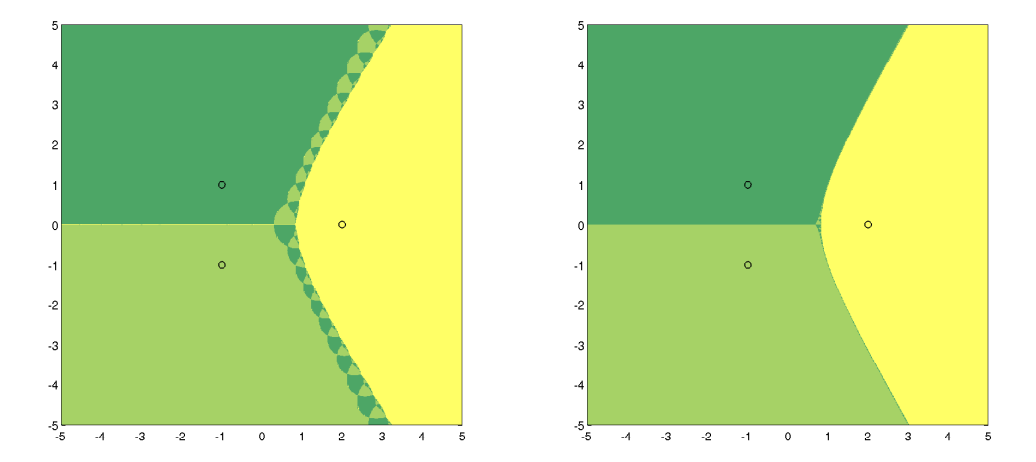

FIGURE 4. Attractors for $z^3 - 2z - 4 = 0$ by the Newton method. On the left with step size control for ($\tau = 0.1$) and on the right for ($\tau = 0.001$).

is located in the same exact attractor as the initial value x_0. To decide whether or not the starting value x_0 approaches the correct zero, we simultaneously compute a reference solution x_{ref} using a fixed step size $t \ll 1$. Our results demonstrate, in contrast to the Newton method with fixed step size, that the rate of convergence in the adaptive approach is nearly quadratic, and that the number of convergent iterations is close to 100%.

TABLE 1. Performance data for Example 3.1 on $[-5,5] \times [-5,5]$.

	Step size $h \equiv 1$	Step size $\equiv 0.72$	Adapt. $\tau = 0.1$
Average nr. of iterations	21.4	27	14
Average step size	1	0.72	0.72
% of convergent iterations	87.7%	92%	96.5%
Average rate $\tilde{\rho}$	1.72	0.945	1.89
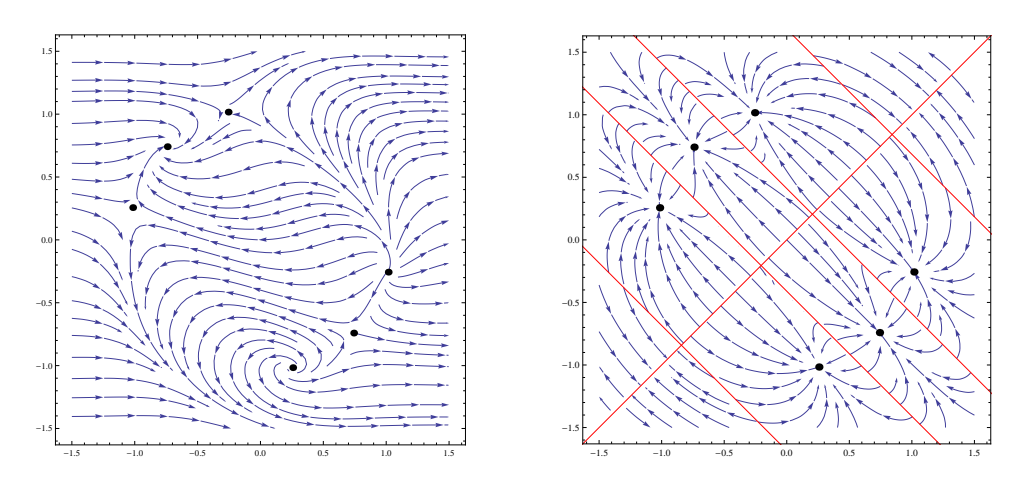
FIGURE 5. The direction field for F resp. of the NRT over the domain $\Omega = [-1.5, 1.5]^2$.

Example 3.2. The second example is a benchmark 2×2 algebraic system from [1]. Consider the function

$$\mathsf{F} : \Omega \subset \mathbb{R}^2 \to \mathbb{R}^2, \qquad \mathsf{F}(x,y) = \begin{pmatrix} \exp(x^2 + y^2) - 3 \\ x + y - \sin(3(x+y)) \end{pmatrix}, \qquad (17)$$

with $\Omega = [-1.5, 1.5]^2$. First of all we notice that the set where the Jacobian of F becomes singular is given by the straight lines

$$\{y = x\}, \quad \text{and} \quad \left\{ y = -x \pm \frac{1}{3} \arccos \left(\frac{1}{3} \right) \pm \frac{2}{3} \pi k, \ k \in \mathbb{N}_{\geq 0} \right\}. \qquad (18)$$

The set Ω contains exactly six different roots of F, which all become locally attractive when applying the NRT; see Figure 5 (right). However, for these six roots, we have six different basins of attraction, which are separated by the straight lines given in (18). In Figure 5 (right) the red lines indicate the critical interfaces where the Jacobian becomes singular.

Before we apply the Newton method to this example let us point out an important fact: The continuous Newton ODE is obviously not able to lead an initial guess x_0 to a root of F when we start in a separated subdomain where no root is located. The present example nicely underlines this effect when we focus on the top right or the bottom left part of the domain Ω (see Figure 5 (right)). In particular, when starting with an initial guess located in a domain where we have no root for F, the corresponding Newton path ends at a critical point. This is potentially different when we apply the discretized version. In fact, starting in a subdomain

without a root does not necessarily imply that the Newton method will be unable to find a root of F since the *discrete* sequence may indeed cross critical interfaces. If we choose $\tau \ll 1$, however, the Newton sequence is close to its corresponding continuous Newton path. This indicates that retaining a certain amount of chaos (i.e., choosing τ not too small) in the discrete Newton iteration might even increase the domain of convergence. This is particularly important when no a priori information on the location of the zeros is available. In Figure 6 we display the domains of attraction. Note that the dark blue shaded part indicates the domain where the iterations fail to converge. We clearly see that step size control is able, on the one hand, to tame the chaotic behavior of the iteration and, on the other hand, to enlarge the domain of convergence. Table 2 presents the performance data for the classical and the adaptive Newton method by sampling 10^4 initial values on the domain $\Omega = [0, 1.5] \times [-1.5, 0]$. Again, the favorable convergence features of the adaptive approach become evident.
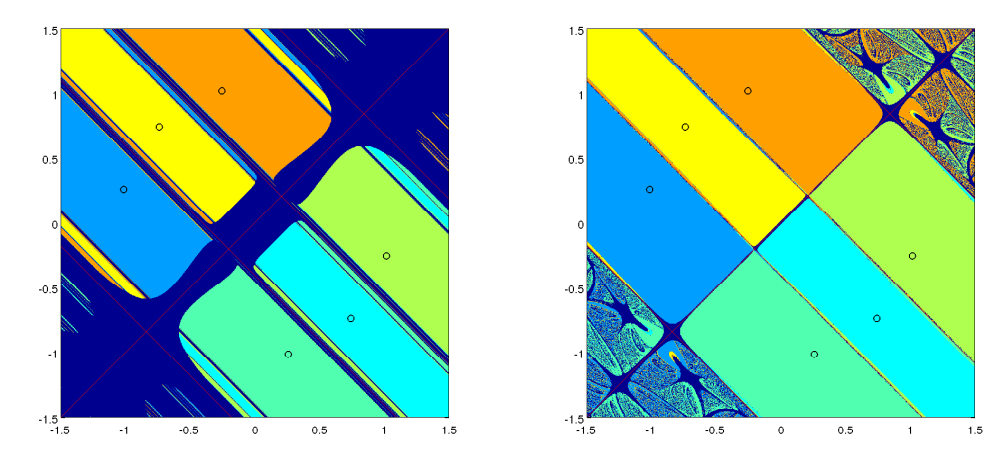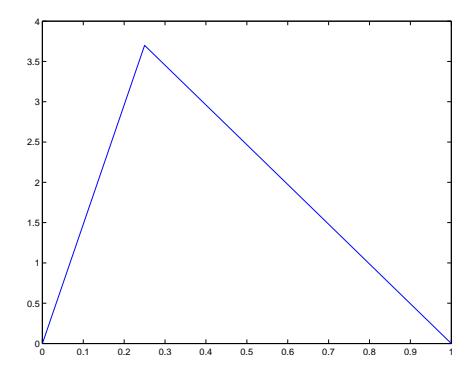

FIGURE 6. Classical Newton method (left) and adaptive Newton method with $\tau = 0.1$ (right).

TABLE 2. Performance data for Example 3.2 on $[0, 1.5] \times [-1.5, 0]$.

	Step size $t \equiv 1$	Step size $t \equiv 0.917$	Adapt. $\tau = 0.1$
Average nr. of iterations	16.7	13.3	6
Average step size	1	0.917	0.917
% of convergent iterations	81%	86%	97%
Average rate $\tilde{\rho}$	1.57	1.11	1.9

3.2. **ODE Boundary Value Examples.** We shall now turn to ordinary boundary value problems.

Example 3.3. As a first example we discuss the nonlinear two-point boundary value problem given by
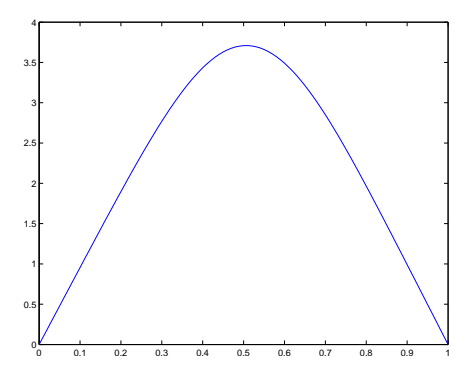
FIGURE 7. Example of initial guess $u_{(i,j,0)}$ (left) and unique positive solution u_+ of (19) (right).

$$\begin{cases} u'' + u^3 = 0, \text{ on } (0,1), \\ u(1) = u(0) = 0. \end{cases} \qquad (19)$$

Let us collect a few facts about (19). Note that if u is a solution, then $-u$ is as well a solution. Moreover, by a phase-plane analysis one can see that (19) has a unique positive solution $u_+ > 0$ (see Figure 7 (right)). Thus, we have (at least) the three solutions $\{u_0, u_+, u_-\}$ with $u_- = -u_+$, and $u_0 \equiv 0$. Note that these solutions are roots of the nonlinear operator $\mathsf{F}(u) = u'' + u^3$. Since, except for the trivial solution, we have no analytical solution formulas at hand, we will compare the numerical solutions and the corresponding exact solutions by means of their integral value over the domain $(0,1)$. Indeed, one can show (see, e.g., [6]) that the unique positive solution u_+ of (19) satisfies

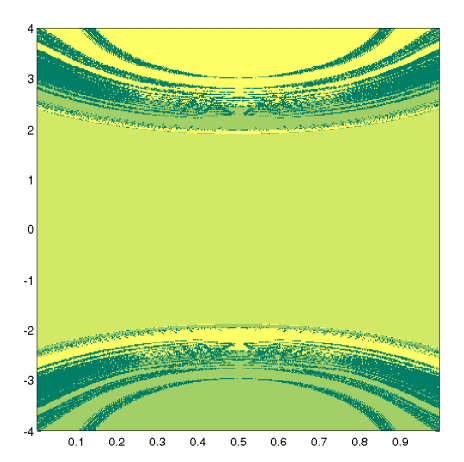$$\int_0^1 u_+(x)\,\mathsf{d}x = \frac{\pi}{\sqrt{2}}.$$

Consequently, we will identify the three solutions above with their corresponding integral values $I_S = \{0, \pi/\sqrt{2}, -\pi/\sqrt{2}\}$.

In our computations we determine numerical solutions of (19) by use of a standard finite element discretization based on piecewise linear basis functions (on uniform meshes with mesh size $h = 1/n$, for some $n \in \mathbb{N}$), and combine it with the Newton scheme (3). Having computed such an approximate solution, we compare its integral value with the three values I_S in order to decide to which solution our initial guess has converged. We will discuss this procedure in more detail in the sequel.

As initial guesses for the Newton iteration we use the following discrete set of piecewise linear continuous functions given by

$$u_{(i,j,0)}(0) = u_{(i,j,0)}(1) = 0, \qquad u_{(i,j,0)}(ih) = \alpha_j, \qquad (20)$$

for $i \in \{1, 2, \ldots, n-1\}$, and $\alpha_j \in [-4, 4]$ with some range of indices for j; cf. Figure 7 (left) for an example. We can now visualize some finite dimensional subsets of the basins of attraction of the three solutions $\{u_0, u_+, u_-\}$ based on these initial guesses. More precisely, we identify an initial guess $u_{i,j,0}$ given in (20) by a point (ih, α_j), where, for the computations, these points are taken from a uniform 400×400 grid in the two-dimensional rectangle $(0,1) \times [-4, 4]$. For each
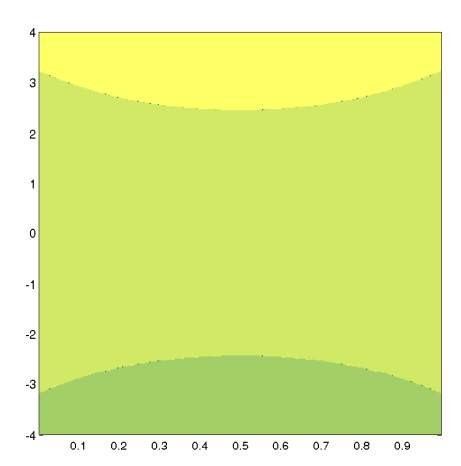
FIGURE 8. The Newton-Galerkin method without (left) and with
(right) step size control ($\tau = 0.1$).

initial guess $u_{i,j,0}$ we compute a sequence of solutions generated by the Newton
method (3), and determine the solution it converges to by checking the correspond-
ing integral value from I_S. The associated starting point (ih, α_j) is then colored
accordingly. This results in a two-dimensional plot showing a subset of the possibly
infinite dimensional attractors of the three solutions.

It is reasonable to expect that the extremum value α_j of the initial guess $u_{(i,j,0)}$
will play an important role in the convergence behavior of the Newton scheme:

(1) For positive values α_j close to the maximum of u_+, we expect that the
    corresponding initial guess $u_{(i,j,0)}$ converges to u_+.
(2) For negative values α_j close to the minimum of u_-, we expect that the
    corresponding initial guess $u_{(i,j,0)}$ converges to u_-.
(3) For values α_j close to 0, we expect that the corresponding initial guess
    $u_{(i,j,0)}$ converges to the trivial solution u_0.

In Figure 8 we present the three basins of attraction associated with the three
solutions $\{u_+, u_-, u_0\}$ for both the traditional Newton-Galerkin scheme (with step
size 1) and for the adaptive Newton-Galerkin method (Algorithm 2.1). For the
standard Newton-Galerkin method, we observe that there is a considerable number
of initial guesses which do not converge to the closest root (close in the sense of
the average value of the exact solution). As in the algebraic example, moving an
initial guess $u_{(i,j,0)}$ to a sufficiently small neighborhood of a solution of (19) might
not always be a well-conditioned procedure. Again, there are initial guesses which
approach the area of quadratic convergence at a low rate or they visit various
attractors before they approach a solution. The dark colored parts in Figure 8
display the initial guesses $u_{(i,j,0)}$ for which the iteration does not converge to one
of the solutions $\{u_0, u_+, u_-\}$ after a prescribed, maximal number of iterations. By
applying step size control in the Newton iteration, we hope for more initial guesses
$u_{i,j,0}$ to converge, and moreover, for the chaotic behavior to be tamed considerably.
This is indeed the case as becomes clear from Figure 8 (right), where we clearly see
that step size control in the case of solving ODEs by the Newton-Galerkin method
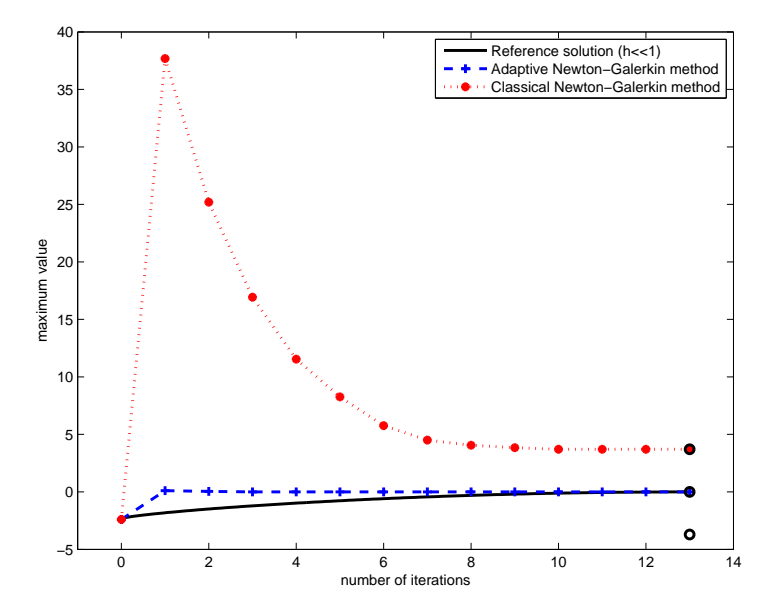is able to reproduce the boundaries between the attractors.

FIGURE 9. Performance of the classical Newton-Galerkin and of the Newton-Galerkin method with adaptive step size control (with $\tau = 0.5$) for the initial guess associated with the point $(0.5, -2.405)$. The vertical axis represents the extremal value of the corresponding iterate. The three small circles indicate the extremal values of the three solutions of (19).

In Figure 9 we display the behavior of the classical Newton-Galerkin and of the adaptive Newton-Galerkin method with $\tau = 0.5$, for the initial guess $u_{i,j,0}$ with $n = 100$, $ih = 0.5$ and $\alpha_j = -2.405$, i.e., corresponding to the point $(0.5, -2.405)$ which belongs to the attractor of u_0. While the adaptive Newton method follows the exact trajectory closely and hence reaches the "correct" solution u_0 of (19), we see that the classical Newton-Galerkin methods approaches the positive solution u_+ instead. This is due a detour taken by the standard Newton method which is caused by an oversized update at the initial step. Also, notice that the adaptive scheme, as compared to the classical method, converges much faster to the associated zero.

In Table 3 we observe the benefits of step size control based on 10^4 initial values of type (20) with $\alpha_j \in [-4, 4]$. Again, an initial value $u_{(i,j,0)}$ is considered convergent if it approaches the "correct solution" of (19), i.e. the solution that is located in the same "exact" attractor as the initial value. The average numbers of iterations listed in Table 3 are determined such that, firstly, we obtain an absolute accuracy of at least 10^{-8} between the n-th and $(n+1)$-th iterates, and, secondly, the absolute error between the reference solution (which we computed with a small step size $t \ll 1$) and the $(n+1)$-th iterate is at least 10^{-3}. As before we compute an empirically determined convergence rate $\tilde{\rho}$, where, incidentally, we only take into account those iterations which are convergent to the correct zero. The error in the n-th iteration is defined by

$$e_n = \min |I_S - I_N(u_{i,j,n})|.$$

where I_N is the integral value of the numerical solution $u_{i,j,n}$ resulting from n New-
ton steps for the initial value $u_{i,j,0}$. We clearly observe a noticeable improvement
in the average convergence rate $\tilde{\rho}$. Moreover almost all initial guesses converge,
and the number of iterations is reduced by approximately 33% compared to the
traditional method.

TABLE 3. Performance data for Example 3.3 for 10^4 initial guesses
of type (20).

	Step size $h \equiv 1$	Adaptive $\tau = 0.1$
Average nr. of iterations	23.5	16
Average step size	1	0.57
% of convergent iterations	74.5%	97%
Average rate $\tilde{\rho}$	1.4	1.53

Example 3.4. As a second example, we consider the equation

$$\begin{cases} u'' + e^{u+1} = 0 \text{ on } (0,1), \\ u(1) = u(0) = 0, \end{cases} \tag{21}$$

which is also known as the 1-D Bratu problem. We have the analytical solutions

$$u(x) = -2\ln\left(\frac{\cosh\left((x - 1/2)\theta/2\right)}{\cosh\left(\theta/4\right)}\right),$$

where θ is determined by the transcendental equation

$$\theta = \sqrt{2e}\cosh\left(\theta/4\right). \tag{22}$$

Note that there are exactly two solutions θ for (22), and hence, we have two solu-
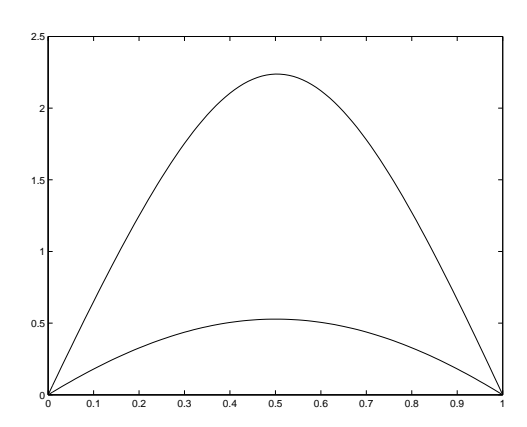tions u_1 and u_2 of (21) (see Figure 10).

FIGURE 10. The two exact solutions u_1, u_2 of Bratu's equation (21).

As initial guesses for the Newton-Galerkin computations we again take the func-
tions defined in (20), and compare the standard method with the one with step size
control. In Figure 11 we present the attractors for the traditional and the adaptive
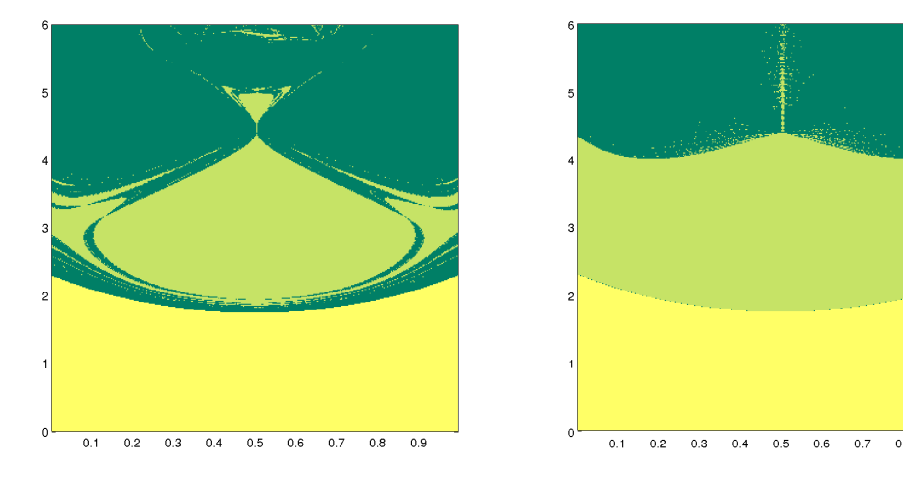
FIGURE 11. The Newton-Galerkin method without (left) and with (right) step size control ($\tau = 0.1$).

Newton-Galerkin methods by sampling 400×400 initial guesses corresponding to the points (ih, α_j) in the rectangular domain $(0, 1) \times [0, 6]$. The yellow and green parts mark the attractors for the solution u_1 and u_2, respectively. We observe that, for the Newton iteration without step size control, there is a dark green shaded part separating the two domains of attraction. However, applying Algorithm 2.1, we observe that the boundaries of the different domains of attraction are nicely smoothed out.

Table 4 is based on the information of 10^4 initial guesses of type (20) with $\alpha_j \in [0, 3]$. Note that the larger average iteration number in the adaptive approach comes from the fact that the classical Newton-Galerkin method breaks down for initial guesses within the dark green shaded part and therefore does not reach the maximal number of iterations. However, note that, employing a step size control procedure, increases the number of convergent initial guesses $u_{(i,0)}$ remarkably.
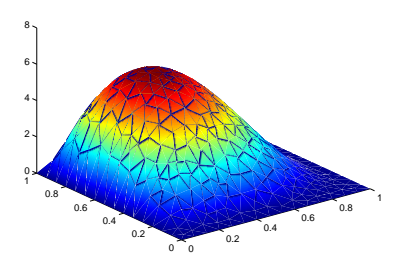
TABLE 4. Performance data for Example 3.4 for 10^4 initial guesses of type (20).

	Step size $\equiv 1$	Adaptive $\tau = 0.1$
Average nr. of iterations	10	14
Average step size	1	0.625
% of convergent iterations	83.5%	98.5%
Average rate $\tilde{\rho}$	1.9	1.2

3.3. **A PDE Boundary Value Example.** We close this application section with a partial differential equation example.

Example 3.5. Consider the boundary value problem

$$\begin{cases} \Delta u + u^3 = 0 \text{ in } \Omega, \\ u = 0, \text{ on } \partial\Omega, \end{cases} \tag{23}$$
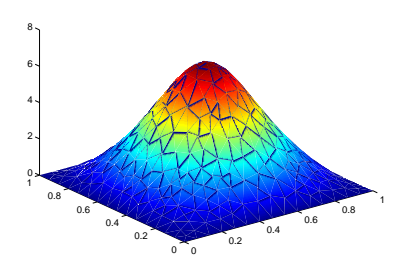
FIGURE 12. Example of an initial guess from (25) (left), and unique positive solution u_+ of (23) (right).

where $\Omega = [0,1]^2$ is the unit square in $\mathbb{R}^2$. Again, we are interested in three particular solutions $\{u_0, u_+, u_-\}$, which are globally zero, positive, and negative on Ω, respectively.

Consider the hill-shaped functions

$$\phi_{(k,j,n)}(x,y) = \left(\frac{x}{x+\varepsilon}\right)^k \left(\frac{y}{y+\varepsilon}\right)^j \left(\frac{1-x}{1-x+\varepsilon}\right)^{n-k} \left(\frac{1-y}{1-y+\varepsilon}\right)^{n-j}, \quad (24)$$
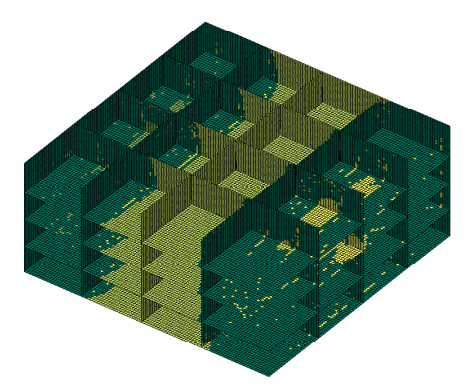
with $\varepsilon = 1/n$. Then, define the initial guesses for the Newton-Galerkin iteration (see Figure 12) as follows: For a fixed $n \in \mathbb{N}$, and $k, j \in \{1, \ldots, n-1\}$, $i \in \{-c, -c+\frac{1}{n}, \ldots, c-\frac{1}{n}, c\}$, with $c \in \mathbb{R}$, we set

$$u_{i,k,j,n} = \frac{i}{\left\|\phi_{(k,j,n)}\right\|_{L^\infty(\Omega)}} \phi_{(k,j,n)}. \quad (25)$$

In Figure 13 we show (finite dimensional subsets of) the attractors of the Newton-Galerkin method without step size control by sampling 10^6 initial guesses (for $c = 8$). As in the ODE case the dark-green shaded parts indicate the initial values which are not convergent to any of the three solutions of Figure 13. For the sake of clarity, we extract three horizontal slices from these plots, namely the one in the middle, at a quarter and on top of the cubes and display them in Figure 13 with resolution 500×500. One can clearly see the chaotic behavior of the classical Newton-Galerkin method; indeed, there are again a large number of initial guesses which do not converge to the closest solution (as in the ODE-case we call an approximate solution close to the exact solution of (23) if it is close in the mean, that is, in the integral sense). In addition, we present the basins of attraction based on step size control with $\tau = 0.1$. As in the previous examples step size control is able to tame the chaotic behavior of the classical Newton method. Moreover, the boundaries of the three different basins of attraction are resolved, and the domain of attraction for the three solutions under consideration is considerably enlarged in the given range.

4. CONCLUSIONS

In this paper we have introduced an adaptive Newton method for (nonlinear) operator equations, $\mathsf{F}(x) = 0$, in Banach spaces. While adaptive Newton methods are popular instruments in the area of numerical optimization, our approach makes use of the dynamical system character of the continuous Newton method,
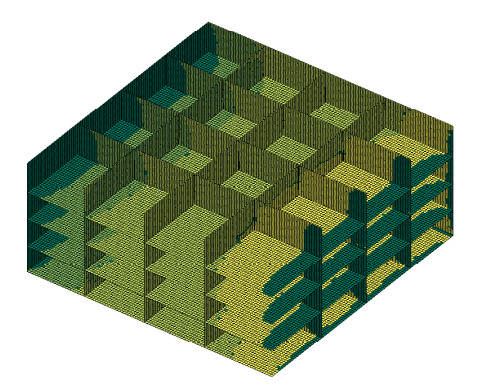
FIGURE 13. Newton-Galerkin method with (left) and without (right) step size control (with $\tau = 0.1$).

$\dot{x} = \mathsf{NF}(x)$. Indeed, this system can be seen as a preconditioned version of the system $\dot{x} = \mathsf{F}(x)$ by $(\mathsf{F}')^{-1}$. It has, on the one hand, the very favorable property of all zeros being attractive, on the other hand, however, singularities in F' may cause the associated discrete system to exhibit chaotic behavior. In order to tame the chaos of the discrete Newton flow, we have proposed a simple, prediction-type, adaptive step size control procedure whose purpose is to follow the flow of the continuous system to a reasonable extent, i.e., in particular, by avoiding to switch between different attractors. We have tested our method in the context of algebraic systems and of finite element discretizations for boundary value problems. The goal of our experiments was to demonstrate empirically that the proposed scheme is indeed capable of taming the chaotic regime of the traditional Newton-Raphson method, at least in the available setting of two-dimensional graphical representations. Our experiments strongly indicate that the adaptive method in this paper performs very well for the examples considered here: in particular, the graphics reveal that fractal attractor boundaries are being smoothed out, high convergence rates can be retained, and the domains of convergence can be enlarged. Our future research will focus on the combination of the proposed approach with adaptive discretization methods for high- or even infinite-dimensional problems.

REFERENCES

[1] P. Deuflhard. *Newtons method for nonlinear problems*. Springer Ser. Comput. Math., 2004.

[2] M. Drexler, I. J. Sobey, and C. Bracher. On the fractal characteristics of a stabilised Newton method. Technical Report NA-95/26, Computing Laboratory, Oxford University, 1995.

[3] B. I. Epureanu and H. S. Greenside. Fractal basins of attraction associated with a damped Newton's method. *SIAM Review*, 40(1):102–109, 1998.

[4] P. Fatou. Sur les équations fonctionnelles (French). *Bull. Soc. Math. France*, 47:161–271, 1919.

[5] G. Julia. Mémoire sur l'iteration des fonctions rationnelles (French). *J. Math. Pure et Appl.*, 8:47–245, 1918.

[6] P. Korman and Y. Li. Generalized averages for solutions of two-point Dirichlet problems. *J. Math. Anal. Appl.*, 239(2):478–484, 1999.

[7] T. Kunio. Continuous Newton-Raphson method for solving an underdetermined system of nonlinear equations. *Nonlinear analysis, theory, methods and applications*, 3(4):495–503, 1979.
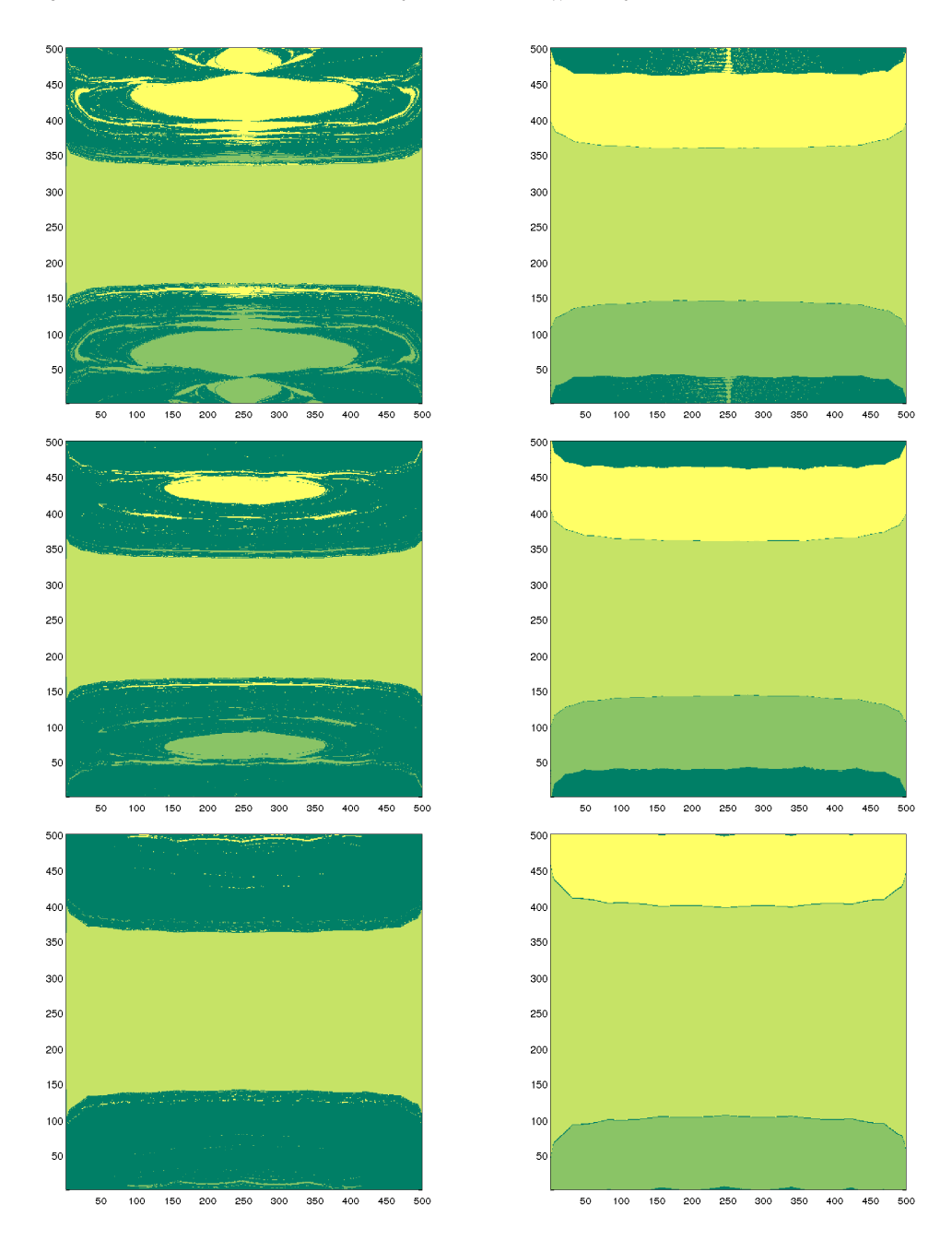
FIGURE 14. Three slices without (left) and with (right) step size control (with $\tau = 0.1$).

[8] T. Kunio. A geometric method in nonlinear programming. *Journal of optimization and applications*, 30(2):181–210, 1980.

[9] J. W. Neuberger. Continuous Newton's method for polynomials. *The Mathematical Intelligencer*, 21(3):18–23, 1999.

[10] J.W. Neuberger. Integrated form of continuous Newton's method. *Lecture notes in Pure and applied. math.*, 234:331–336, 2003.

[11] J.W. Neuberger. The continuous Newton's method, inverse functions and Nash Moser. *Amer. Math. Monthly*, 114:432–437, 2007.

[12] J. Nocedal and S. J. Wright. *Numerical optimization*. Springer Series in Operations Research and Financial Engineering. Springer, New York, second edition, 2006.

[13] H.-O. Peitgen and P. H. Richter. *The Beauty of Fractals*. Springer Verlag, 1986.

[14] H. R. Schneebeli and T. P. Wihler. The Newton-Raphson method and adaptive ODE solvers. *Fractals*, 19(1):87–99, 2011.

[15] S. Smale. On the efficiency of algorithms of analysis. *Bull. Amer. Math. Soc. (N.S.)*, 13(2):87–121, 1985.

[16] J. L. Varona. Graphic and numerical comparison between iterative methods. *Math. Intelligencer*, 24(1):37–46, 2002.

[17] E. Zeidler. *Nonlinear Functional Analysis and its Applications. I*. Springer-Verlag, New York, 1986. Fixed-point theorems.